Showcasing research from Professor Hasegawa's laboratory, Institute for Catalysis, Hokkaido University, Sapporo, Japan, Professor Nozaki's laboratory, Graduate School of Engineering, The University of Tokyo, Tokyo, Japan, and Professor Ema's laboratory, Graduate School of Natural Science and Technology, Okayama University, Okayama, Japan.

Aluminum porphyrins with quaternary ammonium halides as catalysts for copolymerization of cyclohexene oxide and CO_2: metal–ligand cooperative catalysis

Aluminum porphyrins with quaternary ammonium halides showed high catalytic performance (TOF up to 10,000 h^{-1} and TON up to 55,000) for the copolymerization of cyclohexene oxide and CO_2, giving poly(cyclohexene carbonate) with high molecular weight (up to 281,000). Both experimental results and DFT calculations revealed the efficient cooperative actions of the aluminum ion and the quaternary ammonium cation during the polymerization process.

ROYAL SOCIETY OF CHEMISTRY

rsc.li/chemical-science

Check for updates

Aluminum porphyrins with quaternary ammonium halides as catalysts for copolymerization of cyclohexene oxide and CO$_2$: metal–ligand cooperative catalysis†

Jingyuan Deng, [iD] [a] Manussada Ratanasak, [b] Yuma Sako, [c] Hideki Tokuda, [c] Chihiro Maeda, [iD] [c] Jun-ya Hasegawa, [iD] *[b] Kyoko Nozaki [iD] *[a] and Tadashi Ema [iD] ‡*[c]

Bifunctional Al^{III} porphyrins with quaternary ammonium halides, **2-Cl** and **2-Br**, worked as excellent catalysts for the copolymerization of cyclohexene oxide (CHO) and CO$_2$ at 120 °C. Turnover frequency (TOF) and turnover number (TON) reached 10 000 h^{-1} and 55 000, respectively, and poly(cyclohexene carbonate) (PCHC) with molecular weight of up to 281 000 was obtained with a catalyst loading of 0.001 mol%. In contrast, bifunctional Mg^{II} and Zn^{II} counterparts, **3-Cl** and **4-Cl**, as well as a binary catalyst system, **1-Cl** with bis(triphenylphosphine)iminium chloride (PPNCl), showed poor catalytic performances. Kinetic studies revealed that the reaction rate was first-order in [CHO] and [**2-Br**] and zero-order in [CO$_2$], and the activation parameters were determined: $\Delta H^{\ddagger} = 12.4$ kcal mol^{-1}, $\Delta S^{\ddagger} = -26.1$ cal mol^{-1} K^{-1}, and $\Delta G^{\ddagger} = 21.6$ kcal mol^{-1} at 80 °C. Comparative DFT calculations on two model catalysts, Al^{III} complex **2′** and Mg^{II} complex **3′**, allowed us to extract key factors in the catalytic behavior of the bifunctional Al^{III} catalyst. The high polymerization activity and carbonate-linkage selectivity originate from the cooperative actions of the metal center and the quaternary ammonium cation, both of which facilitate the epoxide-ring opening by the carbonate anion to form the carbonate linkage in the key transition state such as **TS3b** ($\Delta H^{\ddagger} = 13.3$ kcal mol^{-1}, $\Delta S^{\ddagger} = -3.1$ cal mol^{-1} K^{-1}, and $\Delta G^{\ddagger} = 14.4$ kcal mol^{-1} at 80 °C).

Introduction

Conversions of CO$_2$ into value-added products are becoming more and more important from the viewpoint of green and sustainable chemistry.[1,2] Among the value-added products, polycarbonates synthesized from epoxides and CO$_2$ have attracted much attention as sustainable and biodegradable materials.[2] Since the discovery of the ring-opening copolymerization of epoxides and CO$_2$ by Inoue in 1969,[3] a variety of metal complex catalysts have been developed,[4–20] such as Co(salen),[4–6] Cr(salen),[7–9] Zn(β-diiminate),[10] and metalloporphyrins.[11,12,20]

Among them, multinuclear metal complexes[4b,6c,9,10b,13–17] and bifunctional monometallic complexes[4a,6b,18–20] have exhibited notable catalytic performances. Among several effective metal elements, aluminum is fascinating from the viewpoint of low toxicity, low price, and abundance on the earth.[2i,11,20]

Previously, we have developed bifunctional Mg^{II} and Zn^{II} porphyrin catalysts, including **3-Br** and **4-Br** (Scheme 1), for the synthesis of cyclic carbonates from epoxides and CO$_2$.[21] The halide anion, the alkyl group, the linker length, and the number and position of the quaternary ammonium halide group were changed, and high catalytic activities were induced by the cooperative action of the metal center (M) and the halide anion (X$^-$); turnover frequencies (TOFs) and turnover numbers (TONs) reached 12 000–46 000 h^{-1} and 103 000–310 000, respectively. However, these Mg^{II} and Zn^{II} complexes showed poor catalytic activity for polycarbonate synthesis.

Here we employed one of the best structures for the synthesis of cyclic carbonates,[21] and replaced the central Mg^{II} or Zn^{II} ion with the Al^{III} ion to prepare new bifunctional catalysts with quaternary ammonium halide groups, **2-Cl** and **2-Br**, for the copolymerization of cyclohexene oxide (CHO) and CO$_2$ (Scheme 1). We used CHO as a monomer despite the low reactivity of the internal epoxide because poly(cyclohexene
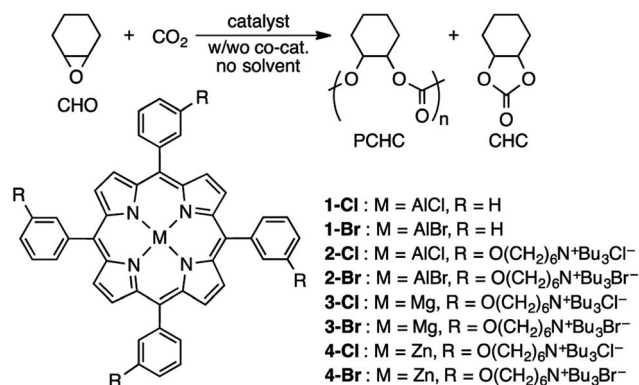
[a]Department of Chemistry and Biotechnology, Graduate School of Engineering, The University of Tokyo, 7-3-1 Hongo, Bunkyo-ku, Tokyo 113-8656, Japan. E-mail: nozaki@chembio.t.u-tokyo.ac.jp

[b]Institute for Catalysis, Hokkaido University, Kita 21, Nishi 10, Kita-ku, Sapporo, Hokkaido 001-0021, Japan. E-mail: hasegawa@cat.hokudai.ac.jp

[c]Division of Applied Chemistry, Graduate School of Natural Science and Technology, Okayama University, Tsushima, Okayama 700-8530, Japan. E-mail: ema@cc.okayama-u.ac.jp

† Electronic supplementary information (ESI) available: Synthesis, copolymerization reactions, kinetic experiments, and DFT calculations. See DOI: 10.1039/d0sc01609h

‡ Cooperative Research Fellow, Institute for Catalysis, Hokkaido University, Japan.

Scheme 1 Copolymerization of CHO and CO_2.

1-Cl : M = AlCl, R = H
1-Br : M = AlBr, R = H
2-Cl : M = AlCl, R = $O(CH_2)_6N^+Bu_3Cl^-$
2-Br : M = AlBr, R = $O(CH_2)_6N^+Bu_3Br^-$
3-Cl : M = Mg, R = $O(CH_2)_6N^+Bu_3Cl^-$
3-Br : M = Mg, R = $O(CH_2)_6N^+Bu_3Br^-$
4-Cl : M = Zn, R = $O(CH_2)_6N^+Bu_3Cl^-$
4-Br : M = Zn, R = $O(CH_2)_6N^+Bu_3Br^-$

carbonate) (PCHC) has promising properties in terms of glass transition temperature and tensile strength.[2] **2-Cl** and **2-Br** showed TOFs of 10 000 h^{-1}, giving PCHC with molecular weight of up to 281 000 with a catalyst loading of 0.001 mol%. DFT calculations suggest that the key transition state in the carbonate-linkage formation step is stabilized by the cooperative effect of (i) the metal activation of the epoxide and (ii) the electrostatic stabilization of the nucleophilic carbonate anion by the quaternary ammonium cation.

Results and discussion

Copolymerization of CHO and CO_2

The copolymerization reactions of CHO with CO_2 (2 MPa) were conducted at 120 °C in the presence of the catalyst without solvent (Table 1). **2-Cl** and **2-Br** showed a TOF of 10 000 h^{-1} (entries 1 and 2). To the best of our knowledge, this is one of the highest values for the solvent-free copolymerization of CHO and CO_2 among monometallic catalysts reported so far.[7,8b,12e] ^{1}H NMR spectra showed a polycarbonate linkage of >99%; PCHC contained no ether linkages, and a trace amount of cyclohexene carbonate (CHC) was detected. Size-exclusion chromatography (SEC) indicated that PCHC had a bimodal molecular weight distribution with a small polydispersity index (PDI) of 1.02,

where the higher-molecular-weight polymers were approximately twice as large as the lower-molecular-weight polymers.[13a] The molecular weight of PCHC exceeded 67 000 in 1 h (entries 1 and 2) and 220 000 in 3 h (entries 3 and 4). When the reaction time was extended to 24 h with a catalyst loading of 0.001 mol% (10 ppm), elastic material capped with a rigid shell was formed, and the reaction appeared to stop owing to the high viscosity of the reaction mixture. Nevertheless, PCHC had a molecular weight of 281 000 or 263 000, corresponding to almost 2000-mers (entries 5 and 6). Although these molecular weights of PCHC are smaller than those calculated by multiplying the TON by the molecular weight of the repeating unit (142), which is due to a chain transfer process,[22,23] the values in Table 1 clearly demonstrate the excellent catalytic performances of **2-Cl** and **2-Br**.

Control experiments were done to address the origin of the high catalytic power of bifunctional Al[III] catalyst **2-Cl**. A binary catalyst system, **1-Cl** with bis(triphenylphosphine)iminium chloride (PPNCl), showed a TOF of 1600 h^{-1}, producing a smaller size of PCHC under otherwise the same reaction conditions (entry 7), which demonstrates the importance of the peripheral quaternary ammonium chlorides in **2-Cl**. On the other hand, the corresponding bifunctional Mg[II] and Zn[II] complexes, **3-Cl** and **4-Cl**, showed TOFs of 27 h^{-1} and 48 h^{-1}, respectively, and low polycarbonate selectivity (52% and 63%) (entries 8 and 9). Clearly, the identity of the central metal ion has a crucial impact on the catalytic process.[24]

Kinetic studies

In kinetic measurements, we used diglyme as a solvent to avoid the generation of a highly viscous or rigid polymer product. To monitor the reaction progress, *in situ* infrared (IR) spectroscopy was employed. Typical examples of the reactions with bifunctional catalyst **2-Br** and binary catalyst system **1-Br**/PPNBr are shown in Fig. 1. The C=O bond stretching signals for PCHC and CHC appear at 1750 cm^{-1} and 1825 cm^{-1}, respectively. The linearity between the IR signal intensity and the amount of PCHC was verified by calibration. **2-Br** was highly selective toward PCHC, and the formation of CHC was not detected at all (Fig. 1a). In contrast, **1-Br**/PPNBr was less selective, and the CHC

Table 1 Copolymerization of CHO and CO_2 with bifunctional catalysts or a binary catalyst system[a]

Entry	Catalyst	S/C	Time (h)	TON[b]	Polycarbonate[b] (%)	M_n[c] (kg mol^{-1})	PDI[c] (M_w/M_n)
1	2-Cl	40 000	1	10 000	>99	68/32	1.02/1.02
2	2-Br	40 000	1	10 000	>99	67/31	1.02/1.02
3	2-Cl	40 000	3	19 200	99	232/106	1.05/1.07
4	2-Br	40 000	3	19 600	99	229/101	1.04/1.08
5[d]	2-Cl	100 000	24	45 000	96	281/96	1.09/1.27
6[e]	2-Br	100 000	24	55 000	97	263/108	1.09/1.12
7[f]	1-Cl	40 000	1	1600	96	3.9/1.6	1.03/1.14
8	3-Cl	40 000	1	27	52	0.41/0.25	1.04/1.02
9	4-Cl	40 000	1	48	63	0.44/0.26	1.06/1.01

[a] Reaction conditions: CHO (2.0 mL, 20 mmol), catalyst (0.0025 mol%), CO_2 (2.0 MPa), 120 °C, in a 50 mL autoclave. [b] TON and the polycarbonate-linkage selectivity were determined by ^{1}H NMR analysis. [c] Determined by size-exclusion chromatography (SEC) analysis using THF as an eluent and polystyrene as a molecular weight standard. Peaks had bimodal shapes. [d] CHO (3.1 mL, 31 mmol), catalyst (0.001 mol%). [e] CHO (3.2 mL, 32 mmol), catalyst (0.001 mol%). [f] PPNCl (4 equiv. of **1-Cl**) was added.
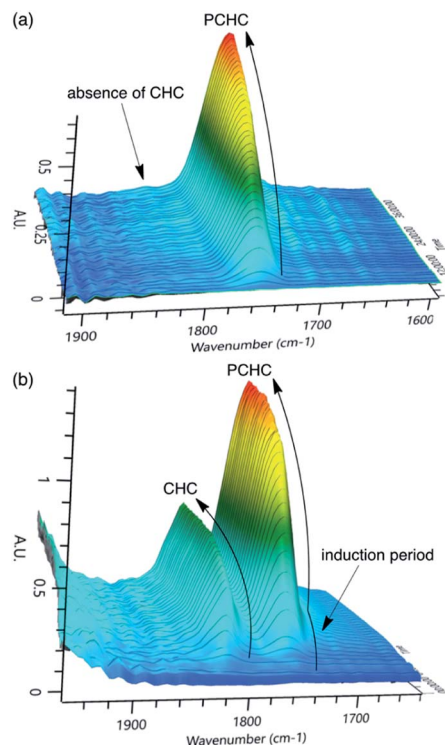
Fig. 1 3D stack plots of *in situ* IR spectra for the copolymerization of CHO and CO_2 in diglyme at 80 °C with (a) **2-Br** and (b) **1-Br**/PPNBr.
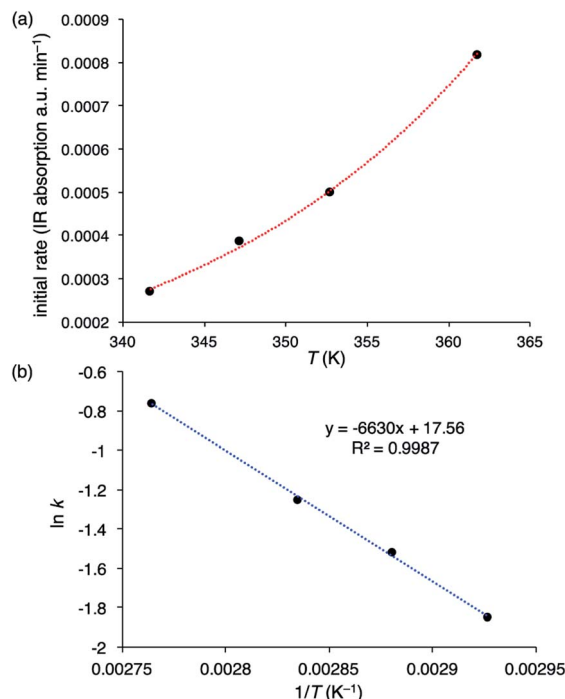

Fig. 2 (a) Plot of initial rates of copolymerization *vs.* temperatures (342, 347, 353, and 362 K) with [**2-Br**] = 0.055 mM, [CHO] = 1.98 M, and a CO_2 pressure of 20 bar in diglyme. (b) Arrhenius plot for the formation of PCHC with **2-Br**.

formation was clearly observed (Fig. 1b). CHC was formed only at the early stage of the copolymerization reaction, and the formation of CHC ceased after a certain reaction time. Accordingly, there was an induction period in the PCHC production, which overlapped with the period of the CHC formation. CHC can be formed easily by the backbiting reaction of the carbonate anion with the C atom attached to the Br atom because bromide is a good leaving group, slowing down the PCHC formation at the outset. Once the polycarbonate linkage is formed, the CHC formation is no longer favored because the resulting alkylcarbonate is a poor leaving group.

Based on the plots of the initial reaction rates at 68 °C *vs.* different concentrations of either CHO, CO_2, or **2-Br** (ESI†), the copolymerization reaction was found to be first-order in both [CHO] and [**2-Br**] and zero-order in [CO_2] in the range of the CO_2 pressure from 10 to 30 bar: $r = k[\text{CHO}]^1[\text{CO}_2]^0[\textbf{2-Br}]^1$, where r and k stand for the reaction rate and the rate constant, respectively. This rate law strongly suggests that the epoxide-ring opening is involved in the rate-determining step, where CO_2 is not involved.

To determine the activation energies (E_a) and activation parameters ($\Delta H^\ddagger$, $\Delta S^\ddagger$, and $\Delta G^\ddagger$), kinetic experiments were conducted at different temperatures. The initial reaction rates for the PCHC formation with **2-Br** are plotted against the reaction temperatures in Fig. 2a, and the Arrhenius plot is shown in Fig. 2b. The activation energy for the PCHC formation was calculated to be 13.2 kcal mol^{-1}. For comparison, the corresponding activation energy with **1-Br**/PPNBr was also determined in the same way to be 16.2 kcal mol^{-1} (ESI†). The Eyring

plot for the PCHC formation with **2-Br** yielded the following activation parameters: $\Delta H^\ddagger = 12.4$ kcal mol^{-1}, $\Delta S^\ddagger = -26.1$ cal mol^{-1} K^{-1}, and $\Delta G^\ddagger = 21.6$ kcal mol^{-1} at 80 °C (ESI†).

Proposed reaction pathway

Based on the results of the kinetic experiments and the rate law, it can be inferred that one equivalent of CHO and **2-Br** are involved in the transition state of the rate-determining step while CO_2 is not involved. A plausible reaction pathway is shown in Scheme 2. First, CHO activated by the metal center in reactant complex **R** is ring-opened by the initiating group (X = Cl or Br) to generate intermediate **I1**. The resulting alkoxide species subsequently undergoes CO_2 insertion to give intermediate **I3a** *via* weak CO_2 adduct **I2**, which should be fast because the reaction is zero-order in [CO_2]. The carbonate anion will dissociate from the metal center to form an ion pair with the tethered quaternary ammonium cation, allowing for the metal coordination of another CHO (**I3b**). This carbonate anion is ready for the nucleophilic attack without diffusing into the bulk solution (Scheme 3a). CHO activated by the metal coordination is ring-opened by the carbonate anion, forming the carbonate linkage (**I4b**). The overall polymerization rate can be substantially improved by accelerating the rate of this ring-opening step. The quaternary ammonium cation in **2** may enhance the nucleophilicity of both the halide anion and the carbonate anion. In addition, the bulky structure of **2** may also prevent the activated CHO from homopolymerization.
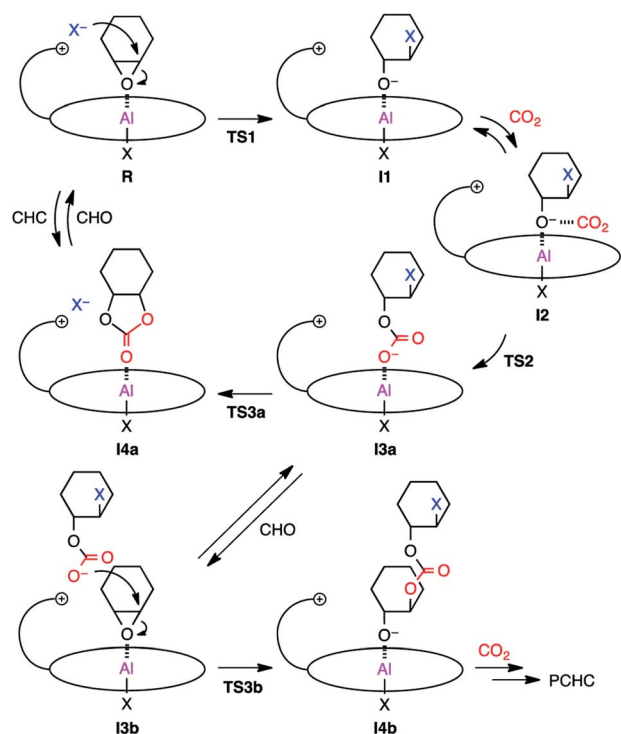
Scheme 2 Plausible reaction pathways for the formation of PCHC and CHC with **2-Cl** or **2-Br**.

On the other hand, a scenario for the binary catalyst system is completely different from that for the bifunctional catalyst. The initiation step will take a longer time because the nucleophilic co-catalyst seldom encounters the catalyst. In addition, the carbonate anion intermediate may dissociate from the metal center to diffuse into the bulk solution, suspending the elongation process (Scheme 3b). The diffused carbonate anion may undergo a backbiting reaction to afford the undesired side product, CHC. Under high dilution conditions, this side reaction is likely to occur, lowering the PCHC selectivity.
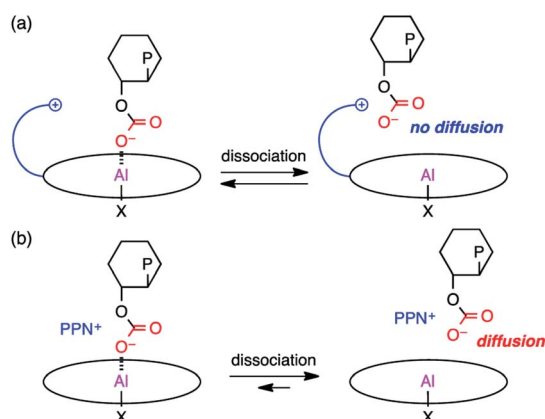
Scheme 3 Roles of the quaternary ammonium cation in (a) bifunctional catalyst **2** and (b) binary catalyst system.

DFT calculations

DFT calculations are powerful tools for the understanding of reaction mechanisms of epoxide/CO_2 copolymerizations.[24,25] Here we performed DFT calculations along the proposed reaction pathway (Scheme 2) using monosubstituted Al^{III} complex **2′** as a model for **2-Br** (Fig. 3). Mg^{II} complex **3′** was also employed as a model for **3-Br** to pursue the origin of the high catalytic activity of Al^{III} complex **2-Br**. The potential energy profiles for the **2′**- and **3′**-catalyzed reactions of CHO with CO_2 are shown in Fig. 3. The structures of the key transition state **TS3b** in the **2′**- and **3′**-catalyzed reactions are shown in Fig. 4, while all of the other transition-state and intermediate structures are given in ESI.†

Fig. 3 clearly indicates that Al^{III} complex **2′** favors the formation of PCHC over that of CHC; the activation energy for **TS3b** ($E_a = 14.6$ kcal mol^{-1}), leading to PCHC, is much smaller than that for **TS3a** ($E_a = 28.3$ kcal mol^{-1}), leading to CHC. This is consistent with the experimental results that PCHC was produced highly selectively with **2-Br** (Table 1). We consider that the carbonate-linkage formation such as **TS3b** is the rate-determining step in the production of PCHC because the energy barrier for **TS3b** ($E_a = 14.6$ kcal mol^{-1}) is greater than that for **TS1** ($E_a = 13.4$ kcal mol^{-1}) and because the carbonate linkages are formed many times in the chain propagation. CO_2 insertion is not the rate-determining step since the energy barrier for **TS2** is very small ($E_a = 7.2$ kcal mol^{-1}), which is consistent with the fact that the reaction rate was independent of the CO_2 pressure (ESI†). The calculated activation parameters of Al^{III} complex **2′** for **TS3b** were as follows: $\Delta H^{\ddagger} = 13.3$ kcal mol^{-1}, $\Delta S^{\ddagger} = -3.1$ cal mol^{-1} K^{-1}, and $\Delta G^{\ddagger} = 14.4$ kcal mol^{-1} at 80 °C. This $\Delta H^{\ddagger}$ value is close to the experimental value for the PCHC formation with **2-Br** ($\Delta H^{\ddagger} = 12.4$ kcal mol^{-1}) although precise comparisons are difficult partly because of the structural differences between **2′** and **2-Br** and between the model and real polymeric substrates.

The activation energy for **TS3a** in the formation of CHC with Mg^{II} complex **3′** ($E_a = 26.3$ kcal mol^{-1}) is much greater than the previously reported value in the **3′**-catalyzed reaction of propylene oxide with CO_2 ($E_a = 17.1$ kcal mol^{-1}).[21b] This is partly because **TS3a** adopts an unfavorable 1,2-diaxial conformation and because the secondary C atom undergoes the nucleophilic attack in the formation of CHC.[25] Interestingly, as compared with Mg^{II} complex **3′**, Al^{III} complex **2′** further disfavors the CHC formation (**TS3a**). This is probably because the stronger Lewis acid (Al^{III}) reduces the nucleophilicity of the carbonate anion. Likewise, **2′** disfavors the CO_2 insertion (**TS2**) as compared with **3′**. In sharp contrast, Al^{III} complex **2′** effectively stabilizes the oxyanion species generating in the epoxide-ring opening steps (**TS1** and **TS3b**) as compared with Mg^{II} complex **3′**. These behaviors can be rationalized by the Lewis acidity of the metal ions: Al^{III} > Mg^{II}. Actually, the most significant difference in the key transition state, **TS3b**, between **2′** and **3′** can be seen around the metal center (Fig. 4); the natural atomic charges on the Al and Mg atoms are +1.86 and +1.71, respectively, and the Al–O and Mg–O distances are 1.85 and 1.99 Å, respectively. Therefore, Al^{III}
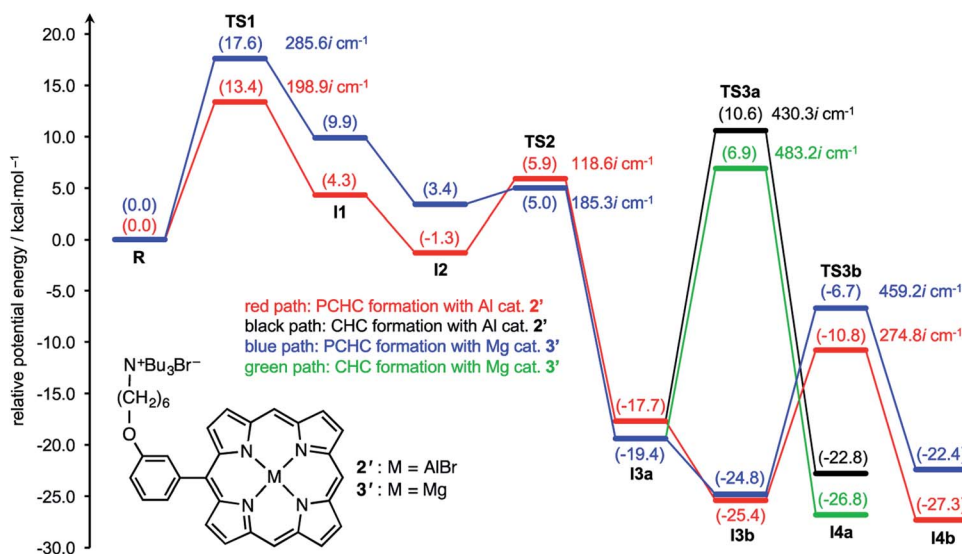
Fig. 3 Potential energy profiles for the **2′** and **3′**-catalyzed reactions of CHO with CO_2. Each transition state and intermediate is designated in the proposed reaction pathway (Scheme 2). Computations were performed at the ωB97XD/6-31G* level with the self-consistent reaction field (SCRF) method (Et_2O). The potential energies relative to reactant complex **R** are given in kcal mol^{-1}. The energies of CO_2 and the second CHO are included in the former steps where they do not appear explicitly in the computational model.

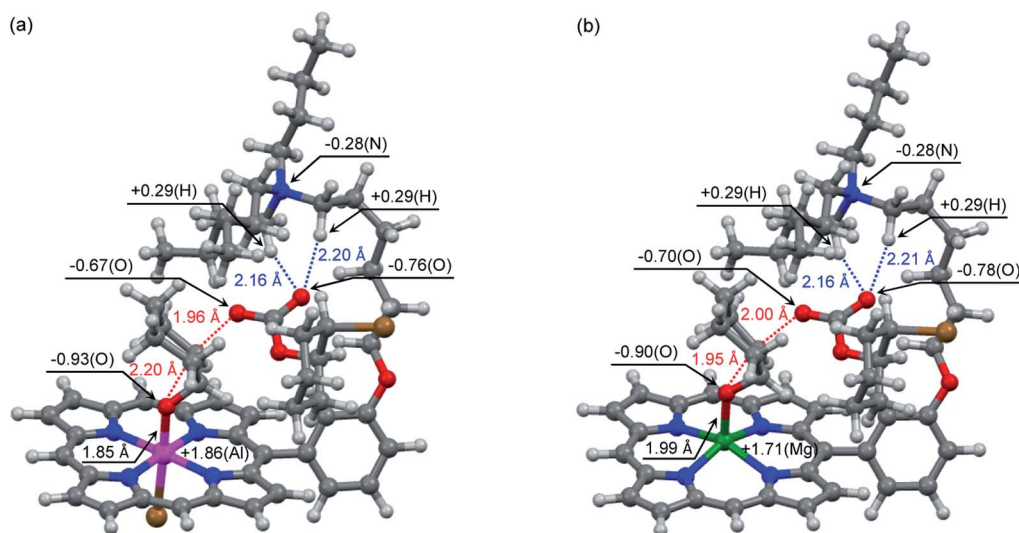**Fig. 4** Optimized structures of transition state **TS3b** in the reaction catalyzed by (a) Al^{III} complex **2′** and (b) Mg^{II} complex **3′**.

complex **2′** can stabilize the negatively charged O atom in **TS3b** more effectively than Mg^{II} complex **3′**.

Previously, it has been proposed that the energy difference in the carbonate–epoxide substitution (**I3a** vs. **I3b** in the present case) is closely related to the chain propagation rate.[24] In other words, a better catalyst has a higher affinity for the epoxide so that the carbonate anion can be replaced more easily by the epoxide, which leads to the efficient chain propagation. Indeed, Fig. 3 indicates that the transition from **I3a** to **I3b** is thermodynamically more favorable with Al^{III} complex **2′** than with Mg^{II} complex **3′**, which accords with the previous proposal.[24]

In addition to the identity of the metal center, the quaternary ammonium cation is also quite important for the

catalysis. Previously, we have reported that the tethered quaternary ammonium cation of bifunctional Mg^{II} complex **3′** undergoes conformational changes to stabilize various anionic species generated during the catalysis for the formation of propylene carbonate.[21b] In this study, we confirmed that all the transition-state and intermediate structures are well stabilized by the tethered quaternary ammonium cation. For example, specific electrostatic interactions between the anionic species and the flexible quaternary ammonium cation can be seen in Fig. 4. In addition, we hypothesized that the tethered quaternary ammonium cation may promote the dissociation of the carbonate anion from the Al atom in **I3a** to give **I3b**.[24] To investigate this possibility, we compared

bifunctional catalyst **2′** with Al^{III} 5-phenylporphyrin complex, having no quaternary ammonium cation, by calculating the energies for the dissociation of the carbonate anion from the Al atom in **I3a** (ESI†). As a result, the carbonate anion was found to dissociate more easily by 18 kcal mol^{-1} in the former case than in the latter case. Furthermore, the tethered quaternary ammonium cation is considered to be useful for the suppression of the diffusion of the growing polymer chain into the bulk solution by means of ion pairing (Scheme 3a). The remaining three quaternary ammonium cations in **2** can contribute to the electrostatic stabilization of the anionic intermediates and transition states. The tethered quaternary ammonium salts in **2** also function as a source of the initiator (X^-). Clearly, the quaternary ammonium halide groups in **2** play multiple essential roles in the highly efficient and selective formation of PCHC.

Conclusions

Copolymerization of epoxides and CO_2 is one of the most straightforward and promising methods for the synthesis of sustainable polymers, polycarbonates. However, only a limited number of metal elements are known to be active for this fascinating transformation. In this work, bifunctional Al^{III} porphyrin complexes with quaternary ammonium halide groups, **2-Cl** and **2-Br**, exhibited excellent catalytic activity and selectivity for the copolymerization of CHO and CO_2. TOF and TON reached 10 000 h^{-1} and 55 000, respectively, and PCHC with molecular weight of up to 281 000 was obtained with a catalyst loading of 0.001 mol%. These excellent catalytic performances of **2-Cl** and **2-Br** resulted from the elaborately designed structures of the bifunctional catalysts with high thermal stability. Kinetic study with *in situ* IR spectroscopy revealed that the copolymerization reaction was first-order in [CHO] and [**2-Br**] and zero-order in [CO_2]: $r = k[CHO]^1[CO_2]^0$[**2-Br**]^1, and the activation parameters were determined by the Arrhenius plot and the Eyring plot: $E_a = 13.2$ kcal mol^{-1}, $\Delta H^{\ddagger} = 12.4$ kcal mol^{-1}, $\Delta S^{\ddagger} = -26.1$ cal mol^{-1} K^{-1}, and $\Delta G^{\ddagger} = 21.6$ kcal mol^{-1} at 80 °C. Comparative DFT calculations on two model catalysts, Al^{III} complex **2′** and Mg^{II} complex **3′**, allowed us to extract key factors in the bifunctional Al^{III} catalyst. Both the Al^{III} metal center and the quaternary ammonium cations work cooperatively to exert high polymerization activity and carbonate-linkage selectivity. The Al^{III} metal center effectively activates the epoxide, and the flexible quaternary ammonium cations simultaneously stabilize and guide the carbonate anion in the key transition state, such as **TS3b** ($E_a = 14.6$ kcal mol^{-1}, $\Delta H^{\ddagger} = 13.3$ kcal mol^{-1}, $\Delta S^{\ddagger} = -3.1$ cal mol^{-1} K^{-1}, and $\Delta G^{\ddagger} = 14.4$ kcal mol^{-1} at 80 °C). In addition, the quaternary ammonium cations in **2-Cl** and **2-Br** are also considered to prevent the anionic intermediates from diffusing into the bulk solution, which enables the efficient copolymerization reaction even with a low catalyst loading of 0.001 mol%. Molecular catalysis utilizing the cooperative effect has recently attracted much attention,[26] and the present work will expand the opportunity of designing further new catalysts in future.

Conflicts of interest

There are no conflicts to declare.

Acknowledgements

Notes and references

1 (a) M. Cokoja, C. Bruckmeier, B. Rieger, W. A. Herrmann and F. E. Kühn, *Angew. Chem., Int. Ed.*, 2011, **50**, 8510; (b) Y. Tsuji and T. Fujihara, *Chem. Commun.*, 2012, **48**, 9956; (c) I. Omae, *Coord. Chem. Rev.*, 2012, **256**, 1384; (d) L. Zhang and Z. Hou, *Chem. Sci.*, 2013, **4**, 3395; (e) M. Aresta, A. Dibenedetto and A. Angelini, *Chem. Rev.*, 2014, **114**, 1709; (f) C. Maeda, Y. Miyazaki and T. Ema, *Catal. Sci. Technol.*, 2014, **4**, 1482; (g) Q. Liu, L. Wu, R. Jackstell and M. Beller, *Nat. Commun.*, 2015, **6**, 5933; (h) G. Fiorani, W. Guo and A. W. Kleij, *Green Chem.*, 2015, **17**, 1375; (i) B. Yu and L.-N. He, *ChemSusChem*, 2015, **8**, 52; (j) Q.-W. Song, Z.-H. Zhou and L.-N. He, *Green Chem.*, 2017, **19**, 3707; (k) S.-S. Yan, Q. Fu, L.-L. Liao, G.-Q. Sun, J.-H. Ye, L. Gong, Y.-Z. Bo-Xue and D.-G. Yu, *Coord. Chem. Rev.*, 2018, **374**, 439.

2 (a) H. Sugimoto and S. Inoue, *J. Polym. Sci., Part A: Polym. Chem.*, 2004, **42**, 5561; (b) D. J. Darensbourg, R. M. Mackiewicz, A. L. Phelps and D. R. Billodeaux, *Acc. Chem. Res.*, 2004, **37**, 836; (c) D. J. Darensbourg, *Chem. Rev.*, 2007, **107**, 2388; (d) S. Klaus, M. W. Lehenmeier, C. E. Anderson and B. Rieger, *Coord. Chem. Rev.*, 2011, **255**, 1460; (e) M. R. Kember, A. Buchard and C. K. Williams, *Chem. Commun.*, 2011, **47**, 141; (f) X.-B. Lu and D. J. Darensbourg, *Chem. Soc. Rev.*, 2012, **41**, 1462; (g) D. J. Darensbourg and S. J. Wilson, *Green Chem.*, 2012, **14**, 2665; (h) X.-B. Lu, W.-M. Ren and G.-P. Wu, *Acc. Chem. Res.*, 2012, **45**, 1721; (i) N. Ikpo, J. C. Flogeras and F. M. Kerton, *Dalton Trans.*, 2013, **42**, 8998; (j) S. Paul, Y. Zhu, C. Romain, R. Brooks, P. K. Saini and C. K. Williams, *Chem. Commun.*, 2015, **51**, 6459; (k) Y. Zhu, C. Romain and C. K. Williams, *Nature*, 2016, **540**, 354; (l) S. J. Poland and D. J. Darensbourg, *Green Chem.*, 2017, **19**, 4990.

3 S. Inoue, H. Koinuma and T. Tsuruta, *J. Polym. Sci., Part B: Polym. Lett.*, 1969, **7**, 287.

4 (a) K. Nakano, T. Kamada and K. Nozaki, *Angew. Chem., Int. Ed.*, 2006, **45**, 7274; (b) K. Nakano, S. Hashimoto and K. Nozaki, *Chem. Sci.*, 2010, **1**, 369; (c) M. Hatazawa,

K. Nakabayashi, S. Ohkoshi and K. Nozaki, *Chem.–Eur. J.*, 2016, **22**, 13677; (*d*) M. Hatazawa, R. Takahashi, J. Deng, H. Houjou and K. Nozaki, *Macromolecules*, 2017, **50**, 7895.

5 (*a*) Z. Qin, C. M. Thomas, S. Lee and G. W. Coates, *Angew. Chem., Int. Ed.*, 2003, **42**, 5484; (*b*) C. T. Cohen, T. Chu and G. W. Coates, *J. Am. Chem. Soc.*, 2005, **127**, 10869.

6 (*a*) X.-B. Lu, L. Shi, Y.-M. Wang, R. Zhang, Y.-J. Zhang, X.-J. Peng, Z.-C. Zhang and B. Li, *J. Am. Chem. Soc.*, 2006, **128**, 1664; (*b*) W.-M. Ren, Z.-W. Liu, Y.-Q. Wen, R. Zhang and X.-B. Lu, *J. Am. Chem. Soc.*, 2009, **131**, 11509; (*c*) Y. Liu, W.-M. Ren, W.-P. Zhang, R.-R. Zhao and X.-B. Lu, *Nat. Commun.*, 2015, **6**, 8594.

7 K. Nakano, M. Nakamura and K. Nozaki, *Macromolecules*, 2009, **42**, 6972.

8 (*a*) D. J. Darensbourg and J. C. Yarbrough, *J. Am. Chem. Soc.*, 2002, **124**, 6335; (*b*) D. J. Darensbourg and R. M. Mackiewicz, *J. Am. Chem. Soc.*, 2005, **127**, 14026; (*c*) D. J. Darensbourg and A. L. Phelps, *Inorg. Chem.*, 2005, **44**, 4622; (*d*) D. J. Darensbourg and A. I. Moncada, *Inorg. Chem.*, 2008, **47**, 10000; (*e*) D. J. Darensbourg, A. I. Moncada, W. Choi and J. H. Reibenspies, *J. Am. Chem. Soc.*, 2008, **130**, 6523; (*f*) D. J. Darensbourg, W.-C. Chung and S. J. Wilson, *ACS Catal.*, 2013, **3**, 3050.

9 S. I. Vagin, R. Reichardt, S. Klaus and B. Rieger, *J. Am. Chem. Soc.*, 2010, **132**, 14367.

10 (*a*) M. Cheng, D. R. Moore, J. J. Reczek, B. M. Chamberlain, E. B. Lobkovsky and G. W. Coates, *J. Am. Chem. Soc.*, 2001, **123**, 8738; (*b*) D. R. Moore, M. Cheng, E. B. Lobkovsky and G. W. Coates, *J. Am. Chem. Soc.*, 2003, **125**, 11911; (*c*) C. M. Byrne, S. D. Allen, E. B. Lobkovsky and G. W. Coates, *J. Am. Chem. Soc.*, 2004, **126**, 11404; (*d*) W. C. Ellis, Y. Jung, M. Mulzer, R. Di Girolamo, E. B. Lobkovsky and G. W. Coates, *Chem. Sci.*, 2014, **5**, 4004; (*e*) F. Auriemma, C. De Rosa, M. R. Di Caprio, R. Di Girolamo, W. C. Ellis and G. W. Coates, *Angew. Chem., Int. Ed.*, 2015, **54**, 1215.

11 (*a*) T. Aida, M. Ishikawa and S. Inoue, *Macromolecules*, 1986, **19**, 8; (*b*) H. Cao, Y. Qin, C. Zhuo, X. Wang and F. Wang, *ACS Catal.*, 2019, **9**, 8669.

12 (*a*) S. Mang, A. I. Cooper, M. E. Colclough, N. Chauhan and A. B. Holmes, *Macromolecules*, 2000, **33**, 303; (*b*) H. Sugimoto and K. Kuroda, *Macromolecules*, 2008, **41**, 312; (*c*) C. E. Anderson, S. I. Vagin, W. Xia, H. Jin and B. Rieger, *Macromolecules*, 2012, **45**, 6840; (*d*) W. Xia, S. I. Vagin and B. Rieger, *Chem.–Eur. J.*, 2014, **20**, 15499; (*e*) R. M. B. Carrilho, L. D. Dias, R. Rivas, M. M. Pereira, C. Claver and A. M. Masdeu-Bultó, *Catalysts*, 2017, **7**, 210.

13 (*a*) F. Jutz, A. Buchard, M. R. Kember, S. B. Fredriksen and C. K. Williams, *J. Am. Chem. Soc.*, 2011, **133**, 17395; (*b*) J. A. Garden, P. K. Saini and C. K. Williams, *J. Am. Chem. Soc.*, 2015, **137**, 15078; (*c*) G. Trott, J. A. Garden and C. K. Williams, *Chem. Sci.*, 2019, **10**, 4618.

14 (*a*) M. W. Lehenmeier, S. Kissling, P. T. Altenbuchner, C. Bruckmeier, P. Deglmann, A.-K. Brym and B. Rieger, *Angew. Chem., Int. Ed.*, 2013, **52**, 9821; (*b*) S. Kissling,

M. W. Lehenmeier, P. T. Altenbuchner, A. Kronast, M. Reiter, P. Deglmann, U. B. Seemann and B. Rieger, *Chem. Commun.*, 2015, **51**, 4579.

15 H. Nagae, R. Aoki, S. Akutagawa, J. Kleemann, R. Tagawa, T. Schindler, G. Choi, T. P. Spaniol, H. Tsurugi, J. Okuda and K. Mashima, *Angew. Chem., Int. Ed.*, 2018, **57**, 2492.

16 M. Cozzolino, K. Press, M. Mazzeo and M. Lamberti, *ChemCatChem*, 2016, **8**, 455.

17 M. Mandal, V. Ramkumar and D. Chakraborty, *Polym. Chem.*, 2019, **10**, 3444.

18 (*a*) E. K. Noh, S. J. Na, S. S, S.-W. Kim and B. Y. Lee, *J. Am. Chem. Soc.*, 2007, **129**, 8082; (*b*) S. S, J. K. Min, J. E. Seong, S. J. Na and B. Y. Lee, *Angew. Chem., Int. Ed.*, 2008, **47**, 7306.

19 J. Liu, W.-M. Ren, Y. Liu and X.-B. Lu, *Macromolecules*, 2013, **46**, 1343.

20 (*a*) X. Sheng, Y. Wang, Y. Qin, X. Wang and F. Wang, *RSC Adv.*, 2014, **4**, 54043; (*b*) W. Wu, X. Sheng, Y. Qin, L. Qiao, Y. Miao, X. Wang and F. Wang, *J. Polym. Sci., Part A: Polym. Chem.*, 2014, **52**, 2346; (*c*) X. Sheng, W. Wu, Y. Qin, X. Wang and F. Wang, *Polym. Chem.*, 2015, **6**, 4719.

21 (*a*) T. Ema, Y. Miyazaki, S. Koyama, Y. Yano and T. Sakai, *Chem. Commun.*, 2012, **48**, 4489; (*b*) T. Ema, Y. Miyazaki, J. Shimonishi, C. Maeda and J. Hasegawa, *J. Am. Chem. Soc.*, 2014, **136**, 15270; (*c*) C. Maeda, T. Taniguchi, K. Ogawa and T. Ema, *Angew. Chem., Int. Ed.*, 2015, **54**, 134; (*d*) C. Maeda, J. Shimonishi, R. Miyazaki, J. Hasegawa and T. Ema, *Chem.–Eur. J.*, 2016, **22**, 6556; (*e*) C. Maeda, S. Sasaki and T. Ema, *ChemCatChem*, 2017, **9**, 946.

22 (*a*) T. Aida and S. Inoue, *Acc. Chem. Res.*, 1996, **29**, 39; (*b*) S. Inoue, *J. Polym. Sci., Part A: Polym. Chem.*, 2000, **38**, 2861; (*c*) D. J. Darensbourg, *Green Chem.*, 2019, **21**, 2214.

23 The MALDI-TOF mass spectrum of PCHC showed a bimodal molecular weight distribution, and peak assignments revealed the structures of the higher- and lower-molecular-weight polymers and a mechanistic aspect involving a chain transfer process (ESI†).

24 T. Ohkawara, K. Suzuki, K. Nakano, S. Mori and K. Nozaki, *J. Am. Chem. Soc.*, 2014, **136**, 10728.

25 (*a*) Z. Liu, M. Torrent and K. Morokuma, *Organometallics*, 2002, **21**, 1056; (*b*) G. A. Luinstra, G. R. Haas, F. Molnar, V. Bernhart, R. Eberhardt and B. Rieger, *Chem.–Eur. J.*, 2005, **11**, 6298; (*c*) M. W. Lehenmeier, C. Bruckmeier, S. Klaus, J. E. Dengler, P. Deglmann, A.-K. Ott and B. Rieger, *Chem.–Eur. J.*, 2011, **17**, 8858; (*d*) A. Buchard, F. Jutz, M. R. Kember, A. J. P. White, H. S. Rzepa and C. K. Williams, *Macromolecules*, 2012, **45**, 6781; (*e*) L. P. Carrodeguas, J. González-Fabra, F. Castro-Gómez, C. Bo and A. W. Kleij, *Chem.–Eur. J.*, 2015, **21**, 6115; (*f*) J. González-Fabra, F. Castro-Gómez, A. W. Kleij and C. Bo, *ChemSusChem*, 2017, **10**, 1233.

26 (*a*) J. R. Khusnutdinova and D. Milstein, *Angew. Chem., Int. Ed.*, 2015, **54**, 12236; (*b*) M. D. Wodrich and X. Hu, *Nat. Rev. Chem.*, 2018, **2**, 99; (*c*) B. D. Nath, K. Takaishi and T. Ema, *Catal. Sci. Technol.*, 2020, **10**, 12.